BMJ Open Diabetes Research & Care

Transcutaneous CO_2 application accelerates fracture repair in streptozotocin-induced type I diabetic rats

Takahiro Oda ,[1] Takahiro Niikura ,[1] Tomoaki Fukui,[1] Keisuke Oe,[1] Yu Kuroiwa,[1] Yohei Kumabe,[1] Kenichi Sawauchi,[1] Ryo Yoshikawa,[1] Yutaka Mifune,[1] Shinya Hayashi,[1] Tomoyuki Matsumoto,[1] Takehiko Matsushita,[1] Teruya Kawamoto,[1] Yoshitada Sakai,[2] Toshihiro Akisue,[3] Ryosuke Kuroda[1]

To cite: Oda T, Niikura T, Fukui T, *et al*. Transcutaneous CO_2 application accelerates fracture repair in streptozotocin-induced type I diabetic rats. *BMJ Open Diab Res Care* 2020;**8**:e001129. doi:10.1136/bmjdrc-2019-001129

► Supplemental material is published online only. To view please visit the journal online (http://dx.doi.org/10.1136/bmjdrc-2019-001129).

This study was presented at the Annual Meeting of the Orthopedic Research Society, 2019, in Austin, Texas (2–5 February 2019), the Annual Meeting of the Orthopedic Research Society, 2020, in Phoenix, Arizona (8–11 February 2020), and the 4th AO Trauma Asia Pacific Scientific Congress, Taipei, Taiwan (24–25 May 2019).

Received 19 December 2019
Revised 29 October 2020
Accepted 11 November 2020

For numbered affiliations see end of article.

Correspondence to
Dr Takahiro Niikura;
tniikura@med.kobe-u.ac.jp

ABSTRACT

Introduction Diabetes mellitus (DM) negatively affects fracture repair by inhibiting endochondral ossification, chondrogenesis, callus formation, and angiogenesis. We previously reported that transcutaneous CO_2 application accelerates fracture repair by promoting endochondral ossification and angiogenesis. The present study aimed to determine whether CO_2 treatment would promote fracture repair in cases with type I DM.

Research design and methods A closed femoral shaft fracture was induced in female rats with streptozotocin-induced type I DM. CO_2 treatment was performed five times a week for the CO_2 group. Sham treatment, where CO_2 was replaced with air, was performed for the control group. Radiographic, histologic, genetic, and biomechanical measurements were taken at several time points.

Results Radiographic assessment demonstrated that fracture repair was induced in the CO_2 group. Histologically, accelerated endochondral ossification and capillary formation were observed in the CO_2 group. Immunohistochemical assessment indicated that early postfracture proliferation of chondrocytes in callus was enhanced in the CO_2 group. Genetic assessment results suggested that cartilage and bone formation, angiogenesis, and vasodilation were upregulated in the CO_2 group. Biomechanical assessment revealed enhanced mechanical strength in the CO_2 group.

Conclusions Our findings suggest that CO_2 treatment accelerates fracture repair in type I DM rats. CO_2 treatment could be an effective strategy for delayed fracture repair due to DM.

Significance of this study

What is already known about this subject?

- Diabetes mellitus (DM) can negatively affect bone fracture healing.
- In studies using a closed femoral shaft fracture model in type I DM rats, delayed fracture healing occurred because of inhibition of endochondral ossification and callus formation.
- Transcutaneous application of CO_2 accelerates fracture repair in a rat fracture model by promoting angiogenesis, blood flow, and endochondral ossification at the fracture site.

What are the new findings?

- Transcutaneous application of CO_2.
- Accelerates fracture healing.
- Reverses the inhibition of cartilage formation, endochondral ossification, bone formation, and mechanical properties that are reported to cause delayed fracture repair in DM.
- Is an easy, less invasive, and potentially effective strategy for patients with delayed fracture repair due to DM.

How might these results change the focus of research or clinical practice?

- Transcutaneous application of CO_2, which is simple and less invasive, could be an effective strategy for patients with delayed fracture repair due to DM.

INTRODUCTION

Diabetes mellitus (DM) is a factor that can negatively affect bone fracture healing. Delayed fracture healing and non-union are more frequent in patients with diabetes, and bony union in such patients often requires a longer period.[1 2] In studies using closed femoral shaft fracture models in DM rats, several authors have demonstrated that delayed fracture healing occurs because of inhibition of endochondral ossification and callus formation.[3 4] In the clinical setting, the number of patients with diabetes is predicted to increase sharply to 693 million worldwide by 2045.[5] Therefore, establishing the causes of delayed fracture healing and developing novel approaches to treat it in patients with diabetes are vital.

We previously designed an easy, non-invasive, topical system for transcutaneous application of CO_2 gas using hydrogel as a novel approach to promote bone fracture healing and continued our investigation for clinical application in fracture treatment. We demonstrated that transcutaneous CO_2

application facilitates O_2 dissociation from hemoglobin via the Bohr effect, thereby promoting oxygenation in the tissues and enhancing local blood flow.[6] Our previous study using a rat femoral fracture model showed that transcutaneous application of CO_2 accelerated fracture repair by promoting angiogenesis, blood flow, and endochondral ossification at the fracture site.[7] Although the detailed molecular or cellular mechanisms are still unclear, transcutaneous CO_2 application might increase vascular endothelial growth factor (VEGF) expression around the fracture site, accelerating the fracture healing process via enhanced angiogenesis.

Therefore, using a diabetic rat fracture model, we aimed to determine whether transcutaneous CO_2 application would promote bone fracture healing in DM by accelerating endochondral ossification and angiogenesis.

RESEARCH DESIGN AND METHODS

Animals

Altogether, 90 female Sprague Dawley rats (SLC Japan, Shizuoka, Japan) with a mean weight (±SD) of 228.4 g (±5.6 g) and 12 weeks old were used in this study. DM rats were created by a single intraperitoneal administration of 40 mg/kg streptozotocin (STZ) (Sigma-Aldrich, St. Louis, MO);[8] the experimental model had type I diabetes. Fractures were induced 2 weeks after STZ administration. Blood glucose levels were measured at the time of fracture creation and sacrifice. Animals with blood glucose levels <300 mg/dL were not recognized as DM rats and were excluded from the study. In this study, we determined the sample size with reference to our previous study.[7]

Surgical procedure

A standard stabilized closed femoral shaft fracture was induced according to previously reported methods.[9] Briefly, retrograde insertion of a 1.25-mm-diameter K-wire into the right femoral intramedullary canal was performed, followed by induction of a closed transverse femoral shaft fracture using a three-point bending apparatus and a drop weight.[9] After creating the fracture, the patellar aponeurosis and the skin were sutured with nylon. Preoperatively, we administered medetomidine (0.15 mg/kg), midazolam (2 mg/kg), and butorphanol (2.5 mg/kg) intraperitoneally for anesthesia and sedation. Postoperatively, we administered benzylpenicillin potassium (200 000 units/kg) intraperitoneally as an antibiotic agent. Unprotected weight bearing was allowed postoperatively. The rats were sacrificed using pentobarbital overdose before the assessments.

Transcutaneous application of CO_2

The animals were randomly divided into two groups: the CO_2 group and the control group (n=45 in each group). Transcutaneous CO_2 was applied to the fractured lower limbs of the rats previously reported.[7] Briefly, after induction of sedation with a minimum dose of isoflurane, the fractured limb was shaved, and hydrogel (NeoChemir, Kobe, Japan), which enhances CO_2 absorption, was applied. The hydrogel (pH 5.5) consisted of carbomer, glycerin, sodium hydroxide, sodium alginate, sodium dihydrogen phosphate, methylparaben, and deionized water. Both limbs were sealed with a polyethylene bag, which was filled with 100% CO_2, for 20 min (online supplemental figure S1). This treatment was performed 5 days a week. The control group received sham treatment, where CO_2 was replaced with air.

Radiographic assessment of fracture repair

The anesthetized rats were fixed in the supine position with the limbs fully extended, and radiographs of the fractured limbs were obtained (n=10 in each group at 1, 2, and 3 weeks after fracture; n=15 in each group at 4 weeks after fracture). Fracture union was defined as the presence of bridging callus formation in at least three of the four cortices on the anteroposterior and lateral views.

Histological assessment for fracture sites

Histological assessment was performed with Safranin-O staining at 1, 2, 3, and 4 weeks after fracture (n=5 in each group). Harvested femurs were fixed in 4% paraformaldehyde at room temperature for 24 hours. Subsequently, femurs were decalcified at room temperature with a decalcifying solution (10% formic acid and 10% formalin; 1:1 ratio) and embedded in paraffin wax. Finally, the femurs were processed to obtain 6-µm sagittal sections using a microtome. The sections were deparaffinized in xylene, dehydrated in a graded alcohol series, stained with Safranin-O/fast green, and detailed histological structures and cartilage areas were visualized using a light microscope. To assess the progression of endochondral ossification, the total cartilage area was calculated using National Institutes of Health (NIH) ImageJ software. The degree of fracture repair was assessed on a five-point scale (grade 0: Pseudoarthrosis formation, grade 1: Incomplete cartilaginous union, grade 2: Complete cartilaginous union, grade 3: Incomplete bony union, grade 4: Complete bony union) according to Allen's grading system.[10]

To evaluate the intrarater interclass correlation coefficient (ICC) and the inter-rater ICC reproducibility, determinations of bone union and scoring of degree of fracture repair by Allen's grading system were performed twice by five surgeons blindly.

Assessment of angiogenesis

At weeks 1, 2, 3, and 4 after fracture, angiogenesis was evaluated (n=5 in each group). To evaluate cross-sectional capillary density, immunofluorescence staining of endothelial cells was performed using fluorescein-labeled isolectin B4 (Vector Laboratories, Burlingame, California, USA). Nuclear staining was performed using 4',6-diamidino-2-phenylindole (DAPI) solution (Nacalai Tesque, Kyoto, Japan). Capillaries were morphometrically examined under a fluorescent microscope. The capillaries in five randomly selected fields in the granulation tissue around the fracture site were counted, and the means were calculated.

Immunohistochemical analysis

Immunohistochemical assessment was performed at 2 weeks and 3 weeks after the fracture (n=5 in each group). We assessed Ki67 expression of chondrocyte within bony callus because it is one of the best-known proliferation markers.[11 12] We also evaluated cathepsin K expression as an osteoclast marker.[13 14] The sections were incubated overnight at 4°C with anti-Ki67 antibody (1:50 dilution, NB500-170, Novus Biologicals, Centennial, Colorado, USA) or anticathepsin K antibody (1:50 dilution, ab19027, Abcam, Cambridge, Massachusetts, USA) and subsequently treated with peroxidase-labeled antimouse immunoglobulin (Histofine Simple Stain MAX PO (R), Nichirei Bioscience, Tokyo, Japan) at room temperature for 60 min. The signal was developed as a brown reaction product using the peroxidase substrate 3,3'-diaminobenzidine (Histofine Simple Stain 3,3′-Diaminobenzidine (DAB) Solution, Nichirei Bioscience). The sections were counterstained with hematoxylin and examined with a BZ-X700 confocal microscope (Keyence Corporation, Osaka, Japan). Immunopositive cells were counted in four random fields under a high-power field.

All morphometric studies of immunofluorescence and immunohistochemical staining were performed by two blinded orthopedic surgeons.

Gene expression assessment and RNA extraction

At weeks 1, 2, 3, and 4 after fracture, the expression of specific genes was measured in five animals in each group by real-time PCR. Newly generated callus tissues around the fracture site were harvested. Tissues were homogenized using TRIzol (Invitrogen, Carlsbad, California, USA) with a T18 ULTRA-TURRAX homogenizer (IKA Werke, Staufen, Germany) immediately after harvesting. Total cellular RNA was extracted from the harvested tissues using the acid guanidinium thiocyanate-phenol-chloroform method and purified using RNeasy Mini Kit (Qiagen, Valencia, California, USA); subsequently, on-column digestion was performed using RNase-free DNase Kit (Qiagen) to prevent contamination with genomic DNA.

Real-time PCR

RNA samples were reverse-transcribed to synthesize single-stranded complementary DNA (cDNA) samples using a high-capacity cDNA reverse transcriptional kit (Applied Biosystems, Foster City, California, USA) according to the manufacturer's instructions. Real-time PCR was performed in duplicate on the cDNA with ABI PRISM 7700 Sequence Detection System and SYBR Green reagent (Applied Biosystems). All primer sequences are shown in online supplemental table S1.

We examined gene expression levels of *collagen II*, collagen *X*, and *matrix metalloproteinase-13 (MMP-13)* to evaluate chondrogenic differentiation; *runt-related transcription factor 2 (Runx2)* and *osterix* was used to evaluate osteogenic differentiation; and *VEGF* was used to evaluate angiogenesis. We evaluated gene expression levels of *tumor necrosis factor-α (TNF-α)*, *macrophage colony-stimulating factor (M-CSF)*, *receptor activator of NF-κB (nuclear factor-kappa B) ligand (RANKL)*, and *a disintegrin and metalloproteinase with thrombospondin motifs 4 (ADAMTS 4)*, all of which have been reported to inhibit fracture healing by being overexpressed in DM.[15 16] We also examined *endothelial nitric oxide synthase (eNOS)*, which contributes to vasodilation function,[17] and *thrombospondin-1 (TSP-1)*, which is a potent endogenous inhibitor of angiogenesis.[18] The expression levels of each gene were first normalized with respect to that of GAPDH (*glyceraldehyde-3-phosphate-dehydrogenase*), which served as an internal control. All results are presented as the fold change relative to one sample of the control group at week 1 (ΔΔCT method; Applied Biosystems).[19]

Biomechanical assessment for fracture repair

A standardized three-point bending test was performed using a load torsion and bending tester at week 4 after fracture (n=5 in each group). The bending force was applied with the crosshead at a speed of 2 mm/min until rupture occurred. Ultimate stress (N), extrinsic stiffness (N/mm), and failure energy (N·mm) were measured.

Statistical analysis

Fisher's exact test was used for radiographic assessment. Histological (degree of fracture repair), fluorescent immunohistochemical, and biomechanical assessments, as well as genetic evaluation with real-time PCR, were performed using the Mann-Whitney U test. The Kruskal-Wallis test with the Bonferroni-corrected post hoc Mann-Whitney U test was used for histological (cartilage area size comparison) and immunohistochemical assessments. P values <0.05 were considered statistically significant. Columns and error bars indicate means and standard errors, respectively. All statistical analyses were carried out using BellCurve for Excel V.3.0 (Social Survey Research Information, Tokyo, Japan).

RESULTS

Radiographic assessment of fracture repair

Representative radiographs of both groups at each time point are shown in figure 1. At week 1, periosteal callus formation was not observed in either the CO_2 or control groups (figure 1A,E). At week 2, bony callus became visible in the CO_2 group but not in the control group (figure 1B,F; white arrows). Bony callus was observed at week 3 in the control group; however, the callus size was not sufficient to form bridging callus even at week 4 (figure 1C,D). At week 3, fracture union with bridging callus formation was achieved in 50% (5/10) of the animals in the CO_2 group and 20% (2/10) in the control group. At week 4, fracture union was achieved in 80% (12/15) in the CO_2 group and 20% (3/15) in the control group. The fracture union rate at week four was significantly higher in the CO_2 group than in the control group ($p<0.05$; figure 1).

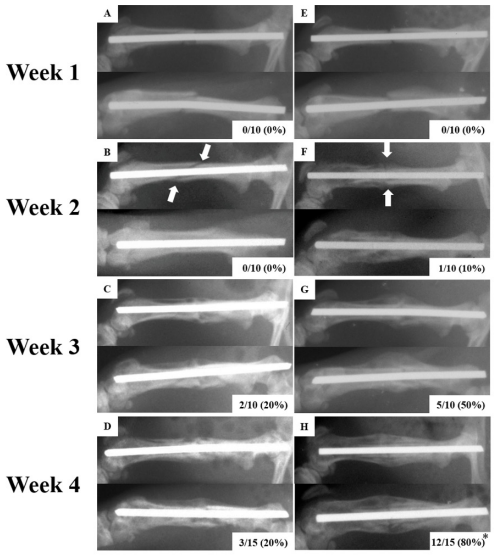

*p < 0.05 compared with the control group

Figure 1 Representative radiographs of fracture repair in the control (A–D) and the CO_2 (E–H) groups. The upper row of each image shows the lateral view, and the lower row shows the anterior-posterior view. The proportion of rats with fracture union is indicated at the lower right of each image.

Histological assessment of fracture sites

Representative histological images are shown in figure 2A. At week 1, cartilage formation was observed between the woven bones in the CO_2 group; by contrast, almost no cartilage area was found in the control group. Cartilage formation in the control group was observed starting at week 2. At week 3, only a small amount of cartilage was observed between the well-generated woven bones in the CO_2 group, while a thick cartilage was observed in the control group. At week 4, bony union was already completed in the CO_2 group, whereas thick cartilage remained in the control group. Woven bone resorption in the CO_2 group indicated the progression of remodeling. Total cartilage area, which was calculated using NIH ImageJ software, was significantly larger in the CO_2 group than in the control group at weeks 1 and 2, indicating that chondrogenesis was promoted in the CO_2 group. The remarkable reduction in total cartilage area in the CO_2 group at weeks 3 and 4 compared with the total cartilage area at week 2 was associated with endochondral ossification progression (figure 2B). The degree of fracture repair according to Allen's grading system was significantly higher in the CO_2 group than in the control group at all time points (figure 2C).

The result of intrarater and the inter-rater ICC reproducibility about determinations of bone union and scoring of degree of fracture repair by Allen's grading system are shown in online supplemental table S2. These results indicated excellent reliability of measurements.

Assessment of angiogenesis

Representative images of immunofluorescence staining with isolectin B4 are shown in figure 2D. The capillary density in the granulation tissue around the fracture site was significantly higher in the CO_2 group than in the control group at all time points (figure 2E).

Immunohistochemical analysis

Representative images of immunohistochemical staining for Ki67 and cathepsin K are shown in figure 3A,C, respectively. At week 2, the percentage of chondrocytes with immunopositive staining for Ki67 was significantly higher in the CO_2 group than in the control group ($p<0.05$). However, this difference disappeared at week 3 (figure 3B). Additionally, in the CO_2 group, the percentage of Ki67-positive chondrocytes dropped significantly from week 2 to week 3 ($p<0.05$).

In the cathepsin K immunohistochemistry, there was no statistically significant difference between the groups in the number of osteoclasts which represented cathepsin K-positive cells in either week 2 or 3 (figure 3D).

Assessment of gene expression

Results of real-time PCR are presented in figure 4. The gene expression levels of *collagen II* and *X* in the CO_2 group were significantly higher than those in the control group at weeks 1, 2, and 3. Gene expression levels of *MMP-13* were significantly higher in the CO_2 group at weeks 2 and 3. Gene expression levels related to osteoblast differentiation were significantly higher in the CO_2 group at weeks 2, 3, and 4 of *Runx2* and at weeks 2 and 3 of *osterix*. VEGF expression levels were significantly greater in the CO_2 group at all time points. Gene expression levels of *TSP-1* were significantly lower in the CO_2 group than in the control group at weeks 3 and 4. No significant differences in *TNF-α* and *RANKL* gene expression levels between the two groups were found at any time point, whereas gene expression levels of *M-CSF* and *ADAMTS 4* were significantly higher in the CO_2 group at weeks 2, 3, and 4. Peak expression of *M-CSF* and *ADAMTS 4*, both of which have been reported to inhibit fracture healing by overexpressing in DM, occurred at week 3 in the CO_2 group.

Biomechanical assessment for fracture repair

All three evaluation items for biomechanical assessment (ie, ultimate stress, extrinsic stiffness and failure energy) were significantly higher in the CO_2 group than in the control group ($p<0.05$; figure 5).

DISCUSSION

DM can delay fracture repair and cause failure of fracture union. Our study showed that transcutaneous CO_2 application accelerated fracture repair even in cases with DM.

DM inhibits the bone fracture repair process by impairing cartilage differentiation in the early phase, delaying endochondral ossification, and reducing biomechanical properties of fracture callus.[20] Nevertheless, the detailed mechanisms by which DM inhibits bone fracture repair remain unclear. To elucidate the molecular mechanisms, various studies using rats with type I diabetes have been conducted.[20 21] Several authors reported that

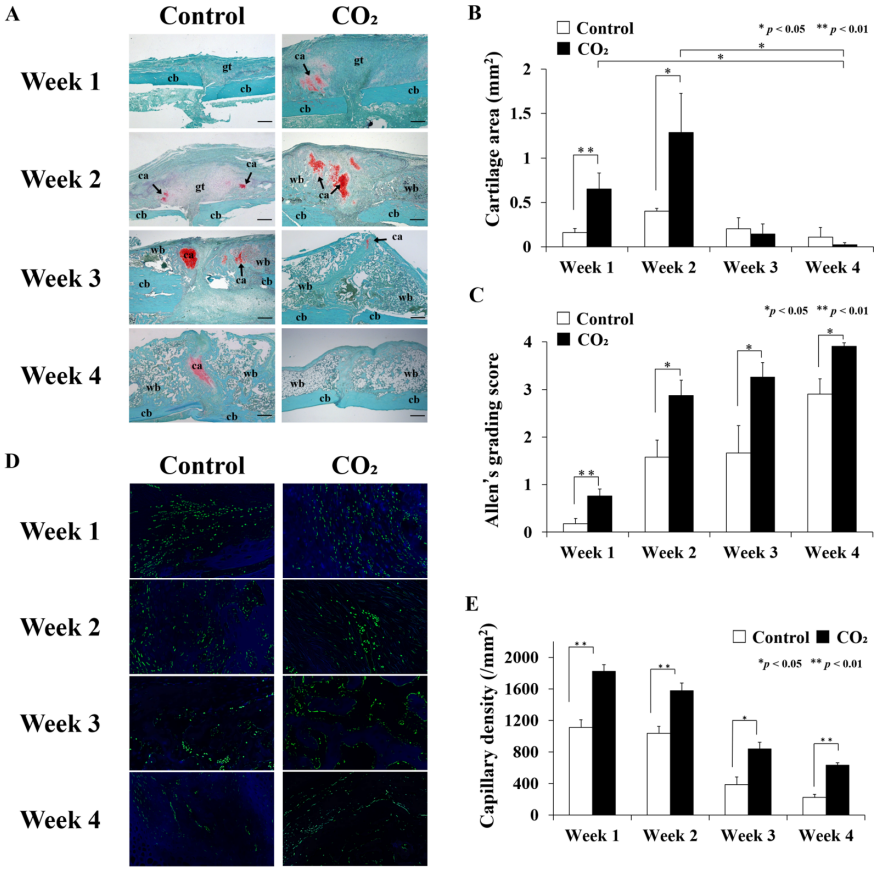

Figure 2 Histological and immunofluorescence assessments of fracture sites in the control and CO_2 groups at weeks 1, 2, 3, and 4 after fracture. (A) Representative histological sections stained with safranin-O/fast green. ca, cartilage; cb, cortical bone; gt, granulation tissue; wb, woven bone; scale bar=500 µm. (B) Changes in the mean area of the cartilage regions, with SE during fracture repair at each time point (n=5 in each group). (C) The degree of fracture repair evaluated by Allen's Grading Score, with SE at each time point. In the CO_2 group, the fracture repair process significantly progressed at all time points (n=5 in each group). (D) Representative images of fluorescent vascular staining in granulation tissue around fracture sites with isolectin B4 (green) and DAPI (blue); scale bar=100 µm. (E) Mean capillary density with SE (n=5 in each group). DAPI, 4',6-diamidino-2-phenylindole.

diabetic rats require a longer time to achieve fracture union than do healthy rats.[22 23] Ogasawara *et al* demonstrated that bone union is achieved at 6 weeks in DM rat femoral fracture model, similar to the model in our study.[4] Moreover, in our study, at 4 weeks after fracture, bone union was achieved in 80% of DM rats in the CO_2 group and in only 20% of the rats in the control group, suggesting that transcutaneous CO_2 application accelerated fracture repair. Histologically, maturation and hypertrophy of chondrocytes are suppressed and remarkably small cartilage callus is formed in DM rats than in healthy rats.[4 24] In this study, although it remains unknown whether the cartilage area of DM rats in the control group was smaller than that of healthy rats, the cartilage area was significantly larger in the CO_2 group than in the control group at weeks 1 and 2, suggesting that chondrocyte differentiation is promoted by transcutaneous CO_2 application. This is consistent with the results of immunohistochemical staining for Ki67, in which the percentage of proliferating cells was significantly higher in the CO_2 group at week 2. Allen's Grading Score, which indicates the degree of fracture repair, was significantly higher in the CO_2 group throughout the fracture repair period. These two histological findings suggest that the fracture repair process is accelerated through the promotion of endochondral ossification by transcutaneous CO_2 application. In the biomechanical assessment, all evaluation items showed significantly greater values in the CO_2 group, and the improvement in the reduction of biomechanical properties due to DM could be associated with the transcutaneous CO_2 application.

Angiogenesis and blood flow at the fracture site are essential factors for fracture repair. In the inflammatory phase of fracture healing, early blood vessel formation supports the invasion of inflammatory cells into the fracture site, and the inflammatory cells release various cytokines that are necessary for fracture repair. Endochondral ossification, which is one of the most important processes in fracture healing, starts during the reparative phase. During this process, avascular cartilaginous tissue is invaded by blood vessels and is transformed into vascular osseous tissue.[7] Therefore, active angiogenesis around the fracture site is indispensable in this phase. Furthermore, sufficient blood flow is essential to

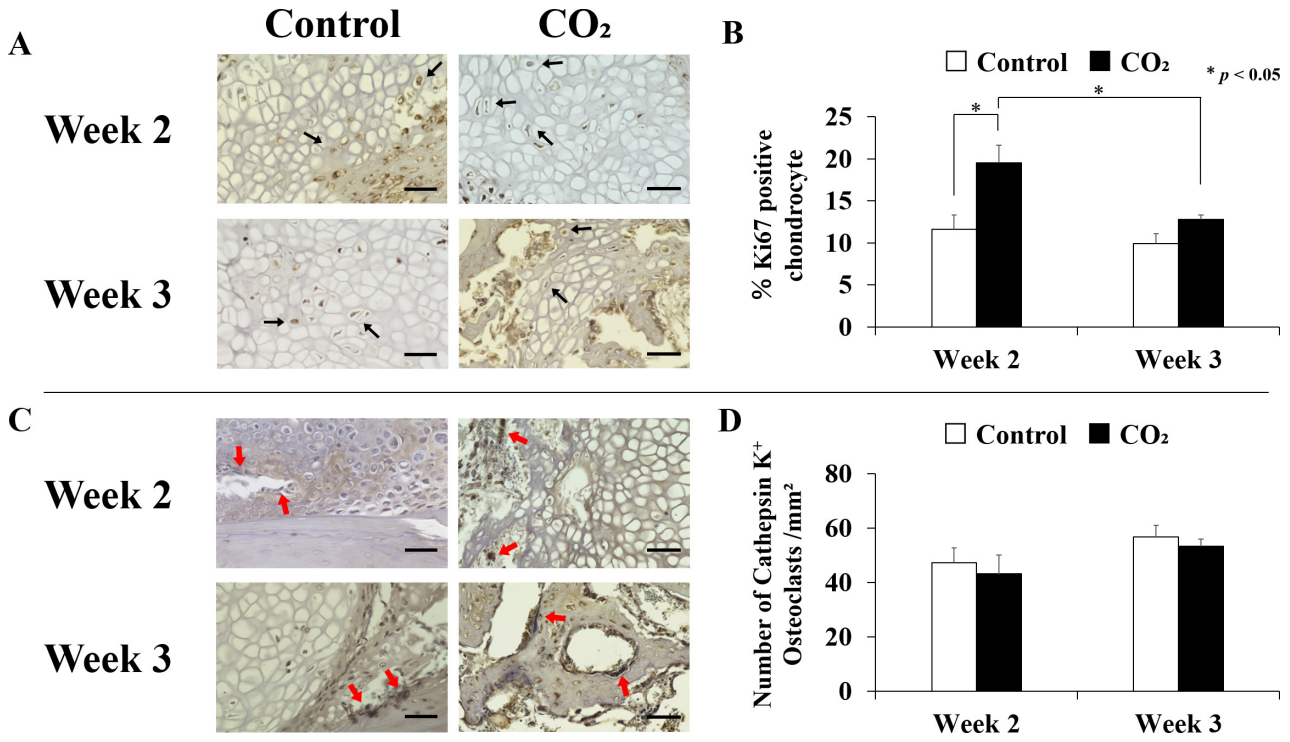

Figure 3 Immunohistochemical assessment of fracture sites in the control and CO_2 groups at weeks 2 and 3 after fracture. (A) Representative images of immunohistochemical staining for Ki67. Black arrows, Ki67-positive chondrocyte; scale bar=50 µm. (B) Changes in the percentage of chondrocytes with immunopositive staining for Ki67, with SE at weeks 2 and 3 (n=5 in each group). (C) Representative images of immunohistochemical staining for cathepsin K. Red arrows, osteoclasts lining both cartilage and bone surface; scale bar=50 µm. (D) Assessment of the number of cathepsin K-positive multinucleated cells counted as osteoclasts per mm² area of the callus.

supply calcium and phosphate that is needed for callus mineralization following endochondral ossification.[25] In a rat experimental model, inhibition of angiogenesis suppressed fracture repair.[26] We previously reported that the capillary density around the fracture site was significantly lower in diabetic rats than in healthy rats.[23] Inhibition of angiogenesis around the fracture site could be a factor of delayed fracture repair in diabetic animals. Various growth factors have been reported to be involved in the fracture repair process. *VEGF* is one of the most important genes associated with angiogenesis, and its expression is essential for normal angiogenesis, callus formation, and mineralization in fracture repair.[25] Lim *et al* reported that diabetes-induced *TNF-α* dysregulation has negative effects on angiogenesis during fracture repair by reducing vessel formation and *VEGF* expression.[27] In the present study, we showed that gene expression levels of *VEGF* in newly generated callus tissue were significantly higher in the CO_2 group at all time points. Fluorescent immunostaining with isolectin B4 revealed that angiogenesis around the fracture site was promoted in the CO_2 group. These results suggest that transcutaneous CO_2 application reverses the reduced gene expression levels of *VEGF* around the fracture site and results in sufficient angiogenesis for fracture repair. We previously reported that transcutaneous CO_2 application increased local oxygen partial pressure via the Bohr effect, resulting in a lower local pH.[5] Acidosis is known to increase gene expression levels of *VEGF*.[28 29] Taken together, these findings suggest that transcutaneous CO_2 application reduces the pH and increases expression levels of *VEGF*.

Transcutaneous CO_2 application increases local blood flow[6 7 30] and therefore has been applied clinically to improve ischemic limb symptoms.[30] Increased blood flow elevates wall shear stress in blood vessels, in turn inducing *eNOS* upregulation.[31 32] *eNOS* is involved in vasodilation and in osteoblast maturation and activity.[33] Other studies found that the activity and expression of *eNOS* were reduced in diabetes and hypoxia,[34 35] and some reports showed that *VEGF* upregulated *eNOS* expression.[36 37] In our study, gene expression levels of *eNOS* were significantly higher in the CO_2 group at weeks 2–4 even in DM rats. *eNOS* expression upregulated by the increased blood flow and the greater expression of *VEGF* possibly contributed to the promotion of fracture repair through vasodilation and maturation and activation of osteoblasts, as previously described. By contrast, gene expression levels of *TSP-1*, which suppresses *VEGF* bioavailability and activity as well as nitric oxide signaling,[38] was significantly lower in the CO_2 group than in the control group at weeks 3 and 4. This result suggests that transcutaneous CO_2 application promotes fracture healing via downregulation of *TSP-1*, which inhibits angiogenesis.

Collagens II and *X* are involved in chondrocyte differentiation, and their gene expression is suppressed in diabetes, resulting in decreased callus size via inhibition

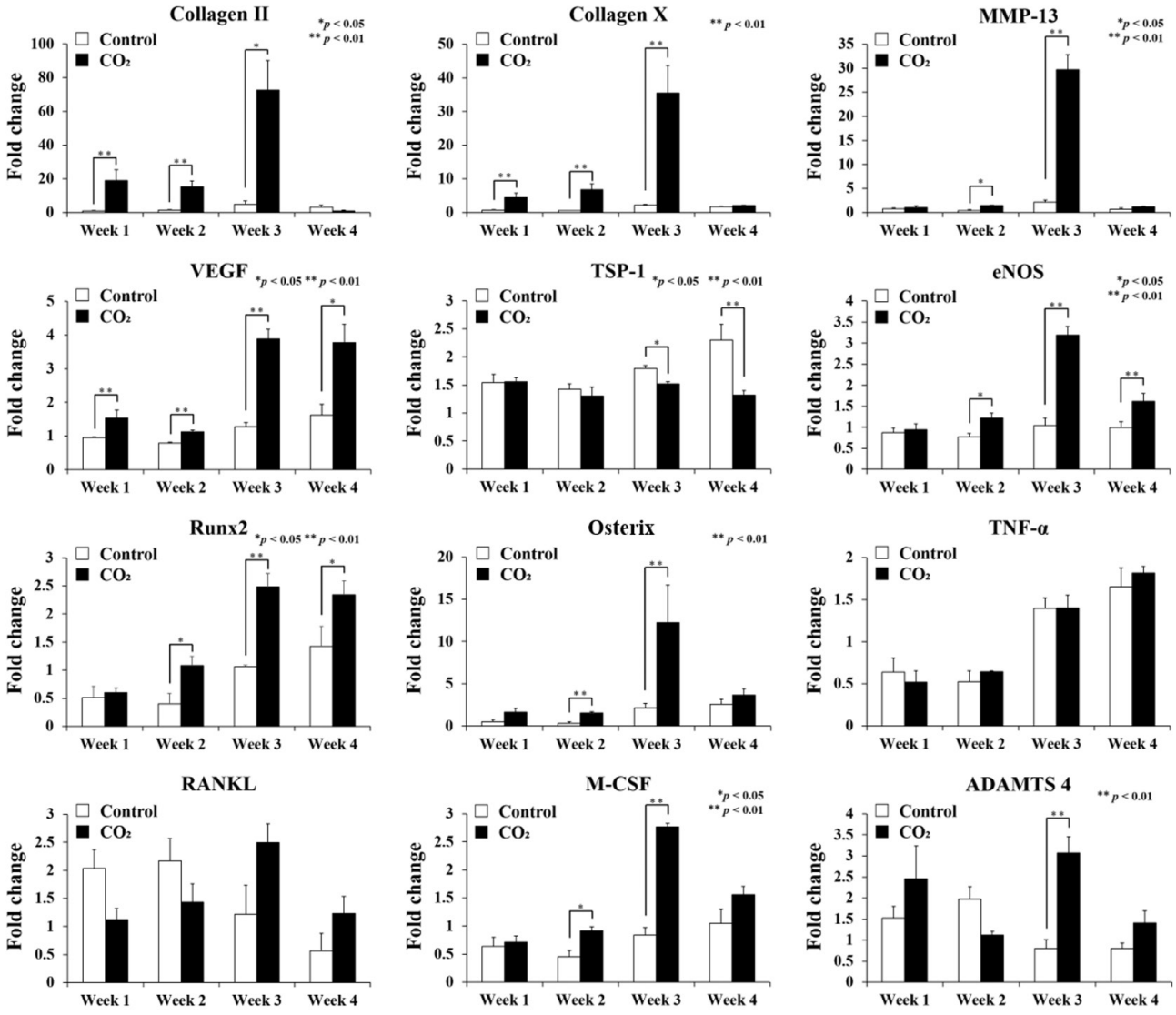

Figure 4 Mean expression with SE of the 12 genes of interest in the control and CO_2 groups at weeks 1, 2, 3, and 4 after fracture, as measured by quantitative real-time PCR (n=5 in each group). Gene expression levels were normalized to GAPDH and are presented as fold change relative to a sample of the control group at week 1. ADAMTS 4, a disintegrin and metalloproteinase with thrombospondinmotifs 4; eNOS, endothelial nitric oxide synthase; GAPDH, glyceraldehyde-3-phosphate-dehydrogenase; M-CSF, macrophage colony-stimulating factor; MMP-13, matrix metalloproteinase-13; RANKL, receptor activator of NF-κB ligand; Runx2, runt-relatedtranscription factor 2; TNF-α, tumor necrosis factor-α; TSP-1, thrombospondin-1; VEGF, vascular endothelial growth factor.

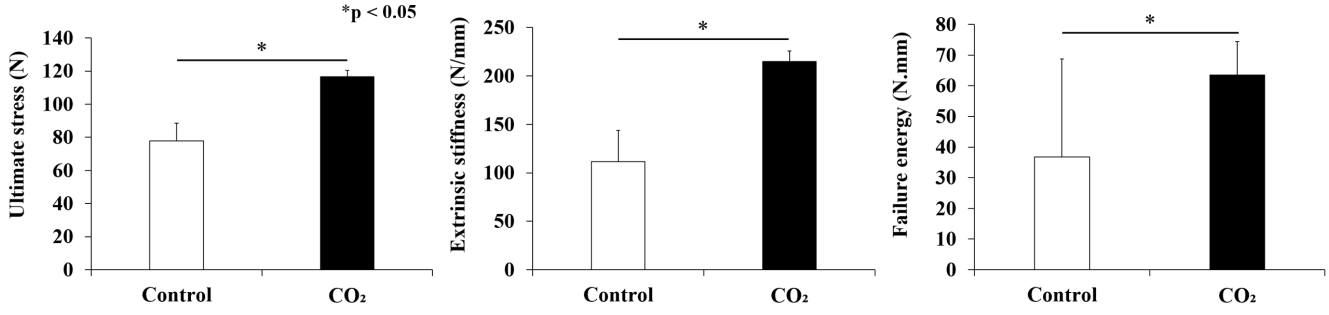

Figure 5 Biomechanical assessment for fracture repair with three-point bending test at week 4 after fracture. Mean values with SE are shown (n=5 in each group).

of chondrocyte differentiation and in reduced mechanical properties.[4 39 40] In the present study, gene expression levels of *collagens II* and *X* were significantly higher in the CO_2 group than in the control group from the early stage of fracture healing to endochondral ossification. These results were consistent with the histological assessment finding that showed significantly larger cartilage formation in the CO_2 group than in the control group at the early stage after fracture creation.

On the other hand, an elevation of the gene expression level of *collagen II* means that chondrocytes are in the proliferative phase, but prolonging this period may trigger delayed fracture healing. In this study, the gene expression level of *collagen II* seemed to peak at week 3 in the CO_2 group, but the difference between weeks 2 and 3 was not statistically significant (Kruskal-Wallis test with the Bonferroni-corrected post hoc Mann–Whitney U test). We also performed immunohistochemical staining for Ki67, which is expressed in the nucleus of proliferating cells and is often used to determine if the cell is in a proliferative or resting phase.[11 12] The percentage of chondrocytes with immunopositive staining for Ki67 was significantly higher in the CO_2 group than in the control group at week 2; however, this difference disappeared at week 3. Additionally, in the CO_2 group, the percentage of Ki67-positive chondrocytes dropped significantly from week 2 to week 3 ($p<0.05$; figure 4). These results indicate that before reaching week 3, the active proliferative phase of chondrocytes, with elevation of gene expression of collagen II, has finished, and the cartilage resorption phase has already begun. We believe this suggests that transcutaneous CO_2 application promoted chondrocyte proliferation at an early time point after fracture.

MMP-13 plays an important role in the maturation of chondrocytes and the induction of angiogenesis. In *MMP-13*-deficient mice, fracture healing was significantly delayed because of inhibition of endochondral ossification.[41] In the present study, gene expression levels of *MMP-13* were significantly higher in the CO_2 group at weeks 2 and 3, corresponding to the endochondral ossification period. This result was consistent with the histological finding that the cartilage area rapidly decreased from week 2 in the CO_2 group because of the progression of endochondral ossification. These genetic and histological results of *collagen II*, *collagen X*, and *MMP-13* suggest that transcutaneous CO_2 application promotes chondrocyte differentiation and endochondral ossification, both of which are suppressed in diabetes, thereby resulting in improved fracture healing.

Runx2 and *osterix* are essential for osteoblast differentiation and both play vital roles in bone formation. *Runx2* induces differentiation of mesenchymal progenitor cells to preosteoblasts, and *osterix* enables preosteoblast differentiation into immature osteoblasts.[42] *Runx2* and osterix are inhibited under hyperglycemic conditions, resulting in impaired bone formation and regeneration.[43 44] In the present study, gene expression levels of both *Runx2* and *osterix* were higher in the CO_2 group at week 2 and later. Although the detailed mechanisms remain unclear, bone formation, which is typically impaired in diabetes, is possibly improved by transcutaneous CO_2 application.

Overexpression of TNF-α and RANKL inhibits fracture healing in diabetes via overactivation of osteoclasts;[15 16] nevertheless, no significant differences in their expression levels were noted between the groups in our study. In addition, immunochemical staining for cathepsin K performed at 2 weeks and 3 weeks after fracture, reported to be the period of excessive increase in the number of osteoclasts in diabetic fracture model animals,[45 46] showed no statistically significant difference in osteoclast numbers between the CO_2 group and the control group. These findings suggest that the promotion of fracture repair by transcutaneous CO_2 application is probably not related to the osteoclast activity regulated by these genes.

M-CSF and *ADAMTS 4* also inhibit fracture repair by the same mechanism as that of TNF-α and *RANKL*;[20 21] however, their expression levels were significantly higher in the CO_2 group than in the control group and peak at week 3 after fracture creation, corresponding to the time when active cartilage resorption in the fracture repair process in rats starts. We speculate that cartilage resorption was promoted in response to the increase in cartilage formation due to transcutaneous CO_2 application.

Delayed fracture healing in patients with DM is a major issue to be solved. Prolonged treatment can lead to increased medical costs, reduce the level of activities of daily living among patients, and cause many complications, such as pneumonia. For this reason, various studies using DM animals have been conducted on promoting fracture healing under the condition of DM.[21 47] However, the need to develop new tools to support fracture healing in DM continues, and the results of our study will be meaningful for fracture patients with DM. Transcutaneous application of CO_2 is relatively safe and easy to perform without invasive surgery; however, clinical application still needs improvement. Ongoing research should be performed to improve the treatment's convenience and safety in clinical settings.

Delayed wound healing and increased susceptibility to infection are also major problems in patients with DM. We believe that increasing blood flow through CO_2 application may accelerate fracture healing and promote wound healing and support efficient local delivery of antibiotics to prevent and treat infection. Several authors have already reported the effects of application of CO_2 on healing of wounds and ulcers.[48 49] Our future studies will investigate the effectiveness of CO_2 application as a support tool for treating wounds or preventing infection in patients with DM.

This study has some limitations. First, because it is difficult to reproduce in vivo conditions, in vitro evaluation could not be performed. Second, we included only rats with type I diabetes. A previous study reported that bone mineral density is decreased in type 1 diabetes but increased in type II diabetes.[50] The detailed mechanisms of delayed fracture repair may differ between type I and

type II diabetes. The number of patients with type II diabetes is greater than those with type I diabetes; therefore, future studies should investigate animals with type II diabetes. Furthermore, whether similar results could be obtained with male rats and other animal species needs to be explored.

In conclusion, we found that transcutaneous application of CO_2 accelerated fracture healing by reversing the inhibition of cartilage formation, endochondral ossification, bone formation, and mechanical properties, all of which are reported to cause delayed fracture repair in DM. We believe this easy and less invasive treatment could be an effective strategy for patients with delayed fracture repair due to DM.

Author affiliations
[1]Orthopaedic Surgery, Kobe University Graduate School of Medicine School of Medicine, Kobe, Hyogo, Japan
[2]Division of Rehabilitation Medicine, Kobe University Graduate School of Medicine School of Medicine, Kobe, Hyogo, Japan
[3]Department of Rehabilitation Science, Kobe University Faculty of Health Sciences and Graduate School of Medicine Faculty of Health Sciences, Kobe, Hyogo, Japan

Acknowledgements The authors thank Ms K Tanaka, Ms M Nagata and Ms M Yasuda (Department of Orthopedic Surgery, Kobe University Graduate School of Medicine) for their excellent technical assistance.

Contributors TO, YuK, YoK, and KS performed the surgeries and radiological examinations. TO performed the histological and genetic examinations. TO and TF analyzed all data, performed the statistical analysis, and were the major contributors in the writing of the manuscript. KO, RY, YM, SH, ToM, TaM, TK, YS, TA, RK, and TN conceived the study and participated in the study design and coordination. All authors read and approved the final manuscript. TN is the guarantor of this work and, as such, had full access to all the data in the study and takes responsibility for the integrity of the data and the accuracy of the data analysis.

Funding This study is funded by Grant-in-Aid for Scientific Research (C) (JSPS KAKENHI Grant Number JP17K10966). The funding source had no role in the study design, data collection and analysis, decision to publish, or preparation of the manuscript.

Competing interests None declared.

Patient consent for publication Not required.

Ethics approval All procedures performed in the animals were in accordance with the ethical standards of the Animal Care and Use Committee of Kobe University Graduate School of Medicine (approval no. P170602-R1).

Provenance and peer review Not commissioned; externally peer reviewed.

Data availability statement Data are available upon reasonable request. All data relevant to the study are included in the article or uploaded as supplemental information.

ORCID iDs
Takahiro Oda http://orcid.org/0000-0002-3223-240X
Takahiro Niikura http://orcid.org/0000-0003-0951-5812

REFERENCES

1 Loder RT. The influence of diabetes mellitus on the healing of closed fractures. *Clin Orthop Relat Res* 1988;232:210–6.
2 Gortler H, Rusyn J, Godbout C, *et al*. Diabetes and healing outcomes in lower extremity fractures: a systematic review. *Injury* 2018;49:177–83.
3 Gandhi A, Beam HA, O'Connor JP, *et al*. The effects of local insulin delivery on diabetic fracture healing. *Bone* 2005;37:482–90.
4 Ogasawara A, Nakajima A, Nakajima F, *et al*. Molecular basis for affected cartilage formation and bone Union in fracture healing of the streptozotocin-induced diabetic rat. *Bone* 2008;43:832–9.
5 Cho NH, Shaw JE, Karuranga S, *et al*. IDF diabetes atlas: global estimates of diabetes prevalence for 2017 and projections for 2045. *Diabetes Res Clin Pract* 2018;138:271–81.
6 Sakai Y, Miwa M, Oe K, *et al*. A novel system for transcutaneous application of carbon dioxide causing an "artificial Bohr effect" in the human body. *PLoS One* 2011;6:e24137.
7 Koga T, Niikura T, Lee SY, *et al*. Topical cutaneous CO2 application by means of a novel hydrogel accelerates fracture repair in rats. *J Bone Joint Surg Am* 2014;96:2077–84.
8 Kawaguchi H, Kurokawa T, Hanada K, *et al*. Stimulation of fracture repair by recombinant human basic fibroblast growth factor in normal and streptozotocin-diabetic rats. *Endocrinology* 1994;135:774–81.
9 Bonnarens F, Einhorn TA. Production of a standard closed fracture in laboratory animal bone. *J Orthop Res* 1984;2:97–101.
10 Allen HL, Wase A, Bear WT. Indomethacin and aspirin: effect of nonsteroidal anti-inflammatory agents on the rate of fracture repair in the rat. *Acta Orthop Scand* 1980;51:595–600.
11 Cardelli M, Zirngibl RA, Boetto JF, *et al*. Cartilage-Specific overexpression of ERRγ results in chondrodysplasia and reduced chondrocyte proliferation. *PLoS One* 2013;8:e81511.
12 Jonquoy A, Mugniery E, Benoist-Lasselin C, *et al*. A novel tyrosine kinase inhibitor restores chondrocyte differentiation and promotes bone growth in a gain-of-function FGFR3 mouse model. *Hum Mol Genet* 2012;21:841–51.
13 Kihara S, Hayashi S, Hashimoto S, *et al*. Cyclin-Dependent kinase inhibitor-1-deficient mice are susceptible to osteoarthritis associated with enhanced inflammation. *J Bone Miner Res* 2017;32:991–1001.
14 Yang X, Ricciardi BF, Hernandez-Soria A, *et al*. Callus mineralization and maturation are delayed during fracture healing in interleukin-6 knockout mice. *Bone* 2007;41:928–36.
15 Kayal RA, Siqueira M, Alblowi J, *et al*. TNF-Alpha mediates diabetes-enhanced chondrocyte apoptosis during fracture healing and stimulates chondrocyte apoptosis through FOXO1. *J Bone Miner Res* 2010;25:1604–15.
16 Alblowi J, Kayal RA, Siqueira M, *et al*. High levels of tumor necrosis factor-alpha contribute to accelerated loss of cartilage in diabetic fracture healing. *Am J Pathol* 2009;175:1574–85.
17 Melikian N, Seddon MD, Casadei B, *et al*. Neuronal nitric oxide synthase and human vascular regulation. *Trends Cardiovasc Med* 2009;19:256–62.
18 Lawler PR, Lawler J. Molecular basis for the regulation of angiogenesis by thrombospondin-1 and -2. *Cold Spring Harb Perspect Med* 2012;2:a006627.
19 Livak KJ, Schmittgen TD. Analysis of relative gene expression data using real-time quantitative PCR and the 2(-Delta Delta C(T)) Method. *Methods* 2001;25:402–8.
20 Park AG, Paglia DN, Al-Zube L, *et al*. Local insulin therapy affects fracture healing in a rat model. *J Orthop Res* 2013;31:776–82.
21 Beam HA, Parsons JR, Lin SS. The effects of blood glucose control upon fracture healing in the BB Wistar rat with diabetes mellitus. *J Orthop Res* 2002;20:1210–6.
22 Takahara S, Lee SY, Iwakura T, *et al*. Altered expression of microRNA during fracture healing in diabetic rats. *Bone Joint Res* 2018;7:139–47.
23 Arakura M, Lee SY, Takahara S, *et al*. Altered expression of SDF-1 and CXCR4 during fracture healing in diabetes mellitus. *Int Orthop* 2017;41:1211–7.
24 Gooch HL, Hale JE, Fujioka H, *et al*. Alterations of cartilage and collagen expression during fracture healing in experimental diabetes. *Connect Tissue Res* 2000;41:81–91.
25 Stegen S, van Gastel N, Carmeliet G. Bringing new life to damaged bone: the importance of angiogenesis in bone repair and regeneration. *Bone* 2015;70:19–27.

26 Hausman MR, Schaffler MB, Majeska RJ. Prevention of fracture healing in rats by an inhibitor of angiogenesis. *Bone* 2001;29:560–4.
27 Lim JC, Ko KI, Mattos M, *et al*. TNFα contributes to diabetes impaired angiogenesis in fracture healing. *Bone* 2017;99:26–38.
28 D'Arcangelo D, Facchiano F, Barlucchi LM, *et al*. Acidosis inhibits endothelial cell apoptosis and function and induces basic fibroblast growth factor and vascular endothelial growth factor expression. *Circ Res* 2000;86:312–8.
29 Xu L, Fukumura D, Jain RK. Acidic extracellular pH induces vascular endothelial growth factor (VEGF) in human glioblastoma cells via ERK1/2 MAPK signaling pathway: mechanism of low pH-induced VEGF. *J Biol Chem* 2002;277:11368–74.
30 Ito T, Moore JI, Koss MC. Topical application of CO2 increases skin blood flow. *J Invest Dermatol* 1989;93:259–62.
31 Toriyama T, Kumada Y, Matsubara T, *et al*. Effect of artificial carbon dioxide foot bathing on critical limb ischemia (Fontaine IV) in peripheral arterial disease patients. *Int Angiol* 2002;21:367–73.
32 Nishida K, Harrison DG, Navas JP, *et al*. Molecular cloning and characterization of the constitutive bovine aortic endothelial cell nitric oxide synthase. *J Clin Invest* 1992;90:2092–6.
33 Baum O, Da Silva-Azevedo L, Willerding G, *et al*. Endothelial NOS is main mediator for shear stress-dependent angiogenesis in skeletal muscle after prazosin administration. *Am J Physiol Heart Circ Physiol* 2004;287:H2300–8.
34 Aguirre J, Buttery L, O'Shaughnessy M, *et al*. Endothelial nitric oxide synthase gene-deficient mice demonstrate marked retardation in postnatal bone formation, reduced bone volume, and defects in osteoblast maturation and activity. *Am J Pathol* 2001;158:247–57.
35 Tousoulis D, Papageorgiou N, Androulakis E, *et al*. Diabetes mellitus-associated vascular impairment: novel circulating biomarkers and therapeutic approaches. *J Am Coll Cardiol* 2013;62:667–76.
36 Liao JK, Zulueta JJ, Yu FS, *et al*. Regulation of bovine endothelial constitutive nitric oxide synthase by oxygen. *J Clin Invest* 1995;96:2661–6.
37 Kroll J, Waltenberger J. VEGF-A induces expression of eNOS and iNOS in endothelial cells via VEGF receptor-2 (KDR). *Biochem Biophys Res Commun* 1998;252:743–6.
38 Shen BQ, Lee DY, Zioncheck TF. Vascular endothelial growth factor governs endothelial nitric-oxide synthase expression via a KDR/Flk-1 receptor and a protein kinase C signaling pathway. *J Biol Chem* 1999;274:33057–63.
39 Gooch HL, Hale JE, Fujioka H, *et al*. Alterations of cartilage and collagen expression during fracture healing in experimental diabetes. *Connect Tissue Res* 2000;41:81–91.
40 Topping RE, Bolander ME, Balian G. Type X collagen in fracture callus and the effects of experimental diabetes. *Clin Orthop Relat Res* 1994;308:220–8.
41 Kosaki N, Takaishi H, Kamekura S, *et al*. Impaired bone fracture healing in matrix metalloproteinase-13 deficient mice. *Biochem Biophys Res Commun* 2007;354:846–51.
42 Komori T. Regulation of osteoblast differentiation by transcription factors. *J Cell Biochem* 2006;99:1233–9.
43 Wu X, Zhang Y, Xing Y, *et al*. High-Fat and high-glucose microenvironment decreases Runx2 and TAZ expression and inhibits bone regeneration in the mouse. *J Orthop Surg Res* 2019;14:55.
44 Fowlkes JL, Bunn RC, Liu L, *et al*. Runt-Related transcription factor 2 (Runx2) and RUNX2-related osteogenic genes are down-regulated throughout osteogenesis in type 1 diabetes mellitus. *Endocrinology* 2008;149:1697–704.
45 Alharbi MA, Zhang C, Lu C, *et al*. FOXO1 deletion reverses the effect of diabetic-induced impaired fracture healing. *Diabetes* 2018;67:2682–94.
46 Kayal RA, Tsatsas D, Bauer MA, *et al*. Diminished bone formation during diabetic fracture healing is related to the premature resorption of cartilage associated with increased osteoclast activity. *J Bone Miner Res* 2007;22:560–8.
47 Jiang H, Wang Y, Meng J, *et al*. Effects of transplanting bone marrow stromal cells transfected with CXCL13 on fracture healing of diabetic rats. *Cell Physiol Biochem* 2018;49:123–33.
48 Li W-P, Su C-H, Wang S-J, *et al*. CO_2 Delivery To Accelerate Incisional Wound Healing Following Single Irradiation of Near-Infrared Lamp on the Coordinated Colloids. *ACS Nano* 2017;11:5826–35.
49 Wollina U, Heinig B, Uhlemann C. Transdermal CO2 application in chronic wounds. *Int J Low Extrem Wounds* 2004;3:103–6.
50 Vestergaard P. Discrepancies in bone mineral density and fracture risk in patients with type 1 and type 2 diabetes--a meta-analysis. *Osteoporos Int* 2007;18:427–44.

Supplementary figure and tables

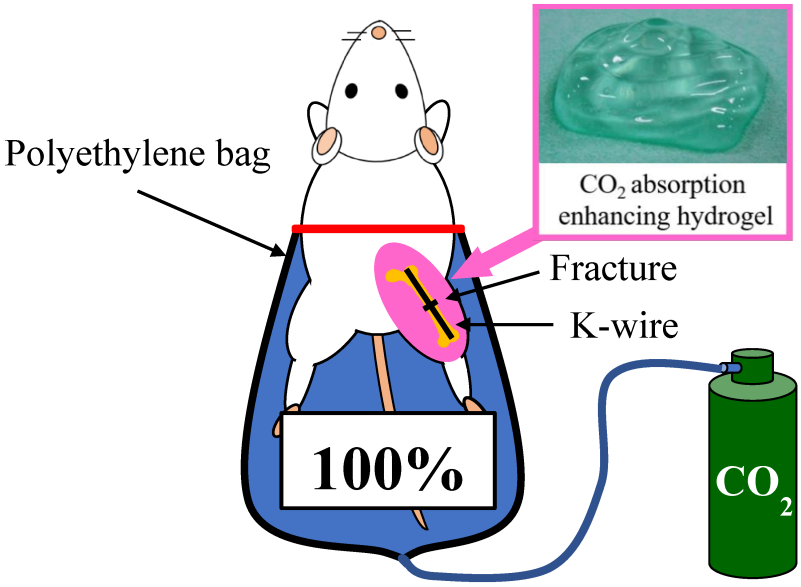

Figure S1. The method of transcutaneous CO_2 application in a rat femoral fracture model.

A standard femoral shaft fracture was created in the right femur and was fixed with an intramedullary Kirschner wire. After the fracture limb was shaved, CO_2 absorption-enhancing hydrogel was applied to the whole fractured limb, and both lower limbs were sealed in a polyethylene bag filled with 100% CO_2 for 20 minutes a day.

Table S1. Specific primers used for real-time PCR amplifications

Gene name	Primer sequence (5'-3')	
	Forward	Reverse
GAPDH	AAATGGTGAAGGTCGGTGTG	TGAAGGGGTCGTTGATGG
Collagen II	GGGCTCCCAGAACATCACCTACCA	TCGGCCCTCATCTCCACATCATTG
Collagen X	GGCAGCAGCACTATGACCCAA	ACAGGCCTACCCAAACGTGAGTCC
MMP-13	CCCTGGAGCCCTGATGTTT	CTCTGGTGTTTTGGGGTGCT
VEGF	TGCACTGGACCCTGGCTTTAC	CGGCAGTAGCTTCGCTGGTAG
TSP-1	GAGTGTCACTGCCAGAACTCA	GTCTGTACTGAAGAGCCCTCA
eNOS	GACCCTCACCGATACAACATAC	CATACAGGATAGTCGCCTTCAC
Runx2	GCGTCAACACCATCATTCTG	CAGACCAGCAGCACTCCATC
Osterix	AGCTCTTCTGACTGCCTGCCTA	TGGGTGCGCTGATGTTTGCT
TNF-α	GCTCACAATGTCTGTGCTTAGAG	GCAGTAGCCACAGCTCCAG
RANKL	AGACACAGAAGCACTACCTGACTC	GGCCCCACAATGTGTTGTA
M-CSF	CGAGGTGTCGGAGCACTGTA	CGATCAACTGCTGCAAAATCTG
ADAMTS 4	CGCTGACCGCCAATGCCAACTG	GCCCAAGGTGAGTGCTTCGTCTG

GAPDH; glyceraldehyde-3-phosphate dehydrogenase, MMP-13; matrix metalloproteinase-13, VEGF; vascular endothelial growth factor, TSP-1; thrombospondin-1, eNOS; endothelial nitric oxide synthase, Runx2; runt-related transcription factor 2, TNF-α; tumor necrosis factor-α, RANKL; receptor activator of NF-κB ligand, M-CSF; macrophage colony-stimulating factor, ADAMTS 4; A disintegrin and metalloproteinase with thrombospondin motifs 4

Table S2. Summary of intra-rater and the inter-rater ICC reproducibility (n = 5 raters)

	Radiographic assessment	Histological assessment
	Determinations of bone union	Scoring of degree of fracture repair
Rater 1 intra-rater reliability	ICC 0.931 (95% CI 0.856–0.967)	ICC 0.980 (95% CI 0.970–0.988)
Rater 2 intra-rater reliability	ICC 0.925 (95% CI 0.844–0.964)	ICC 0.953 (95% CI 0.926–0.970)
Rater 3 intra-rater reliability	ICC 0.893 (95% CI 0.776–0.949)	ICC 0.967 (95% CI 0.948–0.979)
Rater 4 intra-rater reliability	ICC 0.931 (95% CI 0.856–0.967)	ICC 0.990 (95% CI 0.984–0.993)
Rater 5 intra-rater reliability	ICC 0.966 (95% CI 0.930–0.983)	ICC 0.973 (95% CI 0.957–0.982)
Inter-rater reliability	ICC 0.944 (95% CI 0.905–0.971)	ICC 0.950 (95% CI 0.931–0.966)

ICC; inter class correlation coefficient, CI; confidence intervals